Tribology International 130 (2019) 146–154

Contents lists available at ScienceDirect

Tribology International

journal homepage: www.elsevier.com/locate/triboint

Mechanical and tribological evaluation of CrSiCN, CrBCN and CrSiBCN coatings

Qianzhi Wang[a,b,c,*], Fei Zhou[a,b,**], Lian Zhu[a,b], Maoda Zhang[a,b], Jizhou Kong[a,b]

[a] State Key Laboratory of Mechanics and Control of Mechanical Structures, Nanjing University of Aeronautics and Astronautics, Nanjing, 210016, China
[b] College of Mechanical and Electrical Engineering, Nanjing University of Aeronautics and Astronautics, Nanjing, 210016, China
[c] State Key Laboratory of Tribology, Tsinghua University, Beijing, 100084, China

A R T I C L E I N F O

Keywords:
CrCN
Si-B doping
Mechanical properties
Tribological properties

A B S T R A C T

To pinpoint effect of Si-B duplex doping compared to Si and B simplex doping, tribological properties of CrSiCN, CrBCN and CrSiBCN coatings were compared. It was found that CrSiCN coating was still intact after tribotest due to protection of iron oxides from GCr15 counterpart. In contrast, CrBCN coating presented the highest wear rate (4.9×10^{-6} mm^3/Nm) while CrSiBCN coating showed a medium wear rate (2.3×10^{-6} mm^3/Nm). For the same reason, CrSiCN/GCr15 tribopair presented the lowest friction coefficient ($\mu_m = 1.07$) because of low shear strength of iron oxides. CrSiBCN/GCr15 and CrBCN/GCr15 tribopairs presented a higher friction coefficient ($\mu_m = 1.17$ and $\mu_m = 1.43$). The results indicated that Si-B duplex doping was superior to B simplex doping but inferior to Si simplex doping for improving tribological properties.

1. Introduction

In principle, wear resistance of materials is proportional to hardness and hence hard coatings were usually applied on cutting tools to achieve good performance [1–3]. As the next generation of CrN coating, CrCN coating is one of these hard coatings [4,5]. Nevertheless, an inversely proportional relationship between the hardness and wear resistance of CrCN coating was found in literature [6,7]. The same phenomena have also been reported in CrBN [8–10] and CrSiN [11,12] coating systems. It turned out that besides hardness, fracture toughness is another non-ignorable factor to determine the wear resistance of coatings [13,14]. Thus, the toughening of CrCN coatings via element doping (Si and B) was conducted in our previous studies [15–19]. The results showed that CrSiCN coating containing 2.05 at% Si prevented both radial and circumferential cracks under 1000 mN indentation, and therefore presented the lowest wear rate (8.4×10^{-8} mm^3/Nm) in water lubrication [15,16]. In addition, the radial cracks on CrCN coating were inhibited via 27.20 at% B doping, and a wear rate of 2.4×10^{-7} mm^3/Nm was obtained for CrBCN coating sliding against SiC ball in air [17,18].

It has been reported that duplex doping is superior to simplex doping on improving mechanical and tribological properties. For instance, hardness of CrN coating was enhanced to 20.1 GPa via Mo simplex doping but significantly increased to 27.5 GPa via Si-Mo duplex doping. As a consequence, CrMoSiN coating showed a much lower wear rate (7.0×10^{-6} mm^3/Nm) than CrMoN coating (1.6×10^{-5} mm^3/Nm) [20]. Moreover, Wang et al. [21] found that the hardness and fracture toughness of CrTiAlN coating (22.0 GPa and > 3.92 $MPa\cdot\sqrt{m}$) via Ti-Al duplex doping were higher than those of CrTiN coating (13.9 GPa and 2.73 $MPa\cdot\sqrt{m}$) and CrAlN coating (17.7 GPa and 2.70 $MPa\cdot\sqrt{m}$). A similar result with respect to Al simplex doping and Al-Zr duplex doping on CrN coating has also been reported [22]. Thus, based on the optimal characteristics of CrSiCN and CrBCN coatings, Si-B duplex doping, i.e. CrSiBCN coating, is expected to present better mechanical and tribological properties and to be applied on cutting tools, bearings or shafts.

In here, CrSiBCN coating as well as CrSiCN and CrBCN reference coatings were deposited on 316L stainless steel. To pinpoint the effect of Si-B duplex doping, the mechanical and tribological properties of CrSiCN, CrBCN and CrSiBCN coatings were compared and elucidated systematically.

* Corresponding author. State Key Laboratory of Mechanics and Control of Mechanical Structures, Nanjing University of Aeronautics and Astronautics, Nanjing, 210016, China.
** Corresponding author. State Key Laboratory of Mechanics and Control of Mechanical Structures, Nanjing University of Aeronautics and Astronautics, Nanjing, 210016, China.
E-mail addresses: qz.wang@nuaa.edu.cn (Q. Wang), fzhou@nuaa.edu.cn (F. Zhou).

https://doi.org/10.1016/j.triboint.2018.09.025
Received 3 July 2018; Received in revised form 4 September 2018; Accepted 25 September 2018
Available online 26 September 2018

Table 1
Chemical compositions of 316L substrate and GCr15 balls.

Composition	C (wt.%)	Si (wt.%)	Mn (wt.%)	P (wt.%)	S (wt.%)	Ni (wt.%)	Cr (wt.%)	Mo (wt.%)	Cu (wt.%)	Fe (wt.%)
316L	0.02	0.65	1.7	0.03	0.01	12.0	17.5	2.5	–	Balanced
GCr15	0.95	0.25	0.3	0.02	0.01	0.2	1.60	0.1	0.2	Balanced

2. Experimental details

2.1. Coatings deposition

An unbalanced magnetron sputtering system (UDP-650, Teer Coatings Limited) equipped with four cathodes and one ion beam gun was used to deposit CrSiCN, CrBCN and CrSiBCN coatings. Since 316L stainless steel is a common material for friction component manufacturing such as bearings, most of coatings in this study were deposited on 316L stainless steel. Meantime, Si(100) wafers were used as substrate as well for XPS analysis. 316L stainless steel wafers were first polished to a roughness R_a = 30 nm by a precision polishing machine (UNIPOL 802) and then ultrasonically washed with Si(100) wafers together in ethanol before being fixed in deposition chamber. When background pressure was pumped down to 3.0×10^{-6} Torr, 50 sccm Ar was introduced into vacuum chamber to generate Ar^+ via the ion beam gun. Si(100) and 316L stainless steel (composition shown in Table 1) substrates were then bombarded directly by Ar^+ at a bias voltage of −450 V for 30 min. Afterwards, two Cr targets were sputtered (power at 1.2 kW) to deposit a Cr binding layer (200 nm in thickness) at a bias voltage of −80 V and a rotating speed of 10 rpm for 10 min. On top of this Cr binding layer, CrSiCN, CrBCN and CrSiBCN coatings were deposited, and the flow of N_2 was automatically controlled by an optical emission monitor (OEM) preset at 50%. Tetramethylsilane (TMS) was used as Si source for the depositions of CrSiCN and CrSiBCN coatings. All deposition processes were carried out at room temperature and lasted for about 1.2 h to maintain a similar thickness around 2.1 μm. The schematic diagram of deposition system is shown in Fig. 1 and specific deposition parameters are listed in Table 2.

2.2. Structural analyses

The phase patterns of CrSiCN, CrBCN and CrSiBCN coatings were detected using an X-ray diffractometer (Cu Kα radiation, D8-Advance, Bruker). Under a scanning rate of 10°/min, 2θ was scanned from 30° to 80°, and data was analyzed using software Jade5. The chemical compositions and binding conditions of CrSiCN, CrBCN and CrSiBCN coatings were characterized using an X-ray photoelectron spectroscopy (ESCALAB 250, Thermo Scientific). Prior to XPS analysis, CrSiCN, CrBCN and CrSiBCN coatings were pre-etched using Ar^+ bombardment for 4 min. Afterwards, XPS analysis was carried out using an Al-Kα X-ray source (150 W, 20 eV pass energy and 500 μm spot size) with a step size of 0.05 eV Cr2p, Si2p, B1s, C1s and N1s core level spectra were deconvolved using software XPS PEAK 4.1 with a Shirley background type. The binding energy in core level spectra was determined according to XPS database [23]. To compare the effect of Si-B duplex doping with Si simplex doping and B simplex doping, Si and B concentrations in CrSiBCN coating (3.0 and 10.9 at%, respectively) are kept to be similar to Si concentration in CrSiCN coating (4.1 at%) as well as to B concentration in CrBCN coating (10.0 at%). The specific chemical compositions of CrSiCN, CrBCN and CrSiBCN coatings are listed in Table 3.

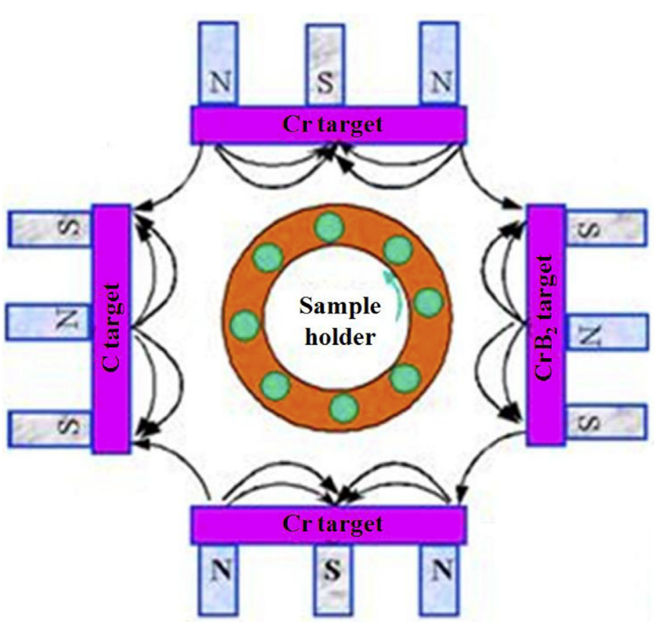

Fig. 1. Schematic diagram of coating deposition system.

2.3. Mechanical evaluation

A nano-indenter equipped with a Berkovich indent was used to measure hardness (*H*) and elastic modulus (*E*) as well as to evaluate the fracture toughness (K_{Ic}) of coatings. With regard to hardness and elastic modulus measurement, a penetration depth of 150 nm was maintained to suppress substrate contribution, and 36 positions on each coating were chosen to carry out test for obtaining reliable data [24,25]. Based on load-unload curve of nano-indentation, elastic recovery R_e could be calculated according to Eq. (1) whilst plastic work W_p could be extracted via integrating load-displacement data.

$$R_e = \frac{h_{max} - h_r}{h_{max}} \tag{1}$$

Where h_{max} and h_r are maximum penetration depth and residual depth after unloading. Both elastic recovery R_e and plastic work W_p are indirect indicator of coatings plasticity.

With regard to fracture toughness, a high load (1000 mN) was applied on each coating to induce crack, and 5 positions on each coating were chosen to ensure repeatability. Afterwards, morphology around indent was observed using a field-emission scanning electron microscope (SIGMA 500, Zeiss). Then, fracture toughness (K_{Ic}) of coatings could be obtained according on Eq. (2) [26,27]:

$$K_{Ic} = \alpha \left(\frac{E}{H}\right)^{0.5} \left(\frac{P}{C_m^{1.5}}\right) \tag{2}$$

In Eq. (2), α is a geometric coefficient correlated to indenter type (0.016 for Berkovich indenter). *P* is applied load (1000 mN) whilst *H* and *E* represent hardness and elastic modulus obtained from the same applied load (1000 mN). C_m is an average length of radial crack based on 15 radial cracks around the five chosen indents.

2.4. Tribological evaluation

Based on the potential application of CrSiCN, CrBCN and CrSiBCN as protective coatings on cutting tools, GCr15 steel as common materials of work pieces (*H* = 7.4 GPa, *E* = 210 GPa, composition in Table 1) was chosen as counterpart. A ball-on-disk tribometer on the